



Dehydration of 1,2-propanediol to propionaldehyde over zeolite catalysts

Dazhi Zhang, Sami A.I. Barri, David Chadwick*

Department of Chemical Engineering, Imperial College London, South Kensington Campus, London SW7 2AZ, UK

ARTICLE INFO

Article history:

Received 11 November 2010
Received in revised form 19 April 2011
Accepted 21 April 2011
Available online 28 April 2011

Keywords:

1,2 Propanediol
Dehydration
Propionaldehyde
Glycerol
Zeolite
Catalyst

ABSTRACT

Dehydration of 1,2-propanediol has been investigated over a range of zeolite catalysts with different pore structures and acidity. The reaction forms part of a two-step process for the conversion of glycerol to propionaldehyde. The effects of reaction temperature, concentration, space velocity, and $\text{SiO}_2/\text{Al}_2\text{O}_3$ ratio have been studied. The medium pore size, unidirectional channel zeolites ZSM-23 and Theta-1 showed high activity and selectivity to propionaldehyde (exceeding 90 wt% at 300–350 °C). Selectivity to the intermolecular dehydration product 2-ethyl-4-methyl-1,3-dioxolane was high at lower temperatures for all the zeolites, but decreased to a low value at higher temperatures and lower GHSV. The results are discussed in relation to the reaction mechanism and zeolite structures. Significant deactivation was observed for higher 1,2-propanediol partial pressures, which was partially mitigated by the addition of steam.

© 2011 Elsevier B.V. All rights reserved.

1. Introduction

Biomass conversion to fuels and chemicals has been developing quickly [1–3]. The utilization of biomass improves security of energy supply and as a renewable resource it benefits the environment by lowering the overall CO_2 emissions. Nowadays glycerol is produced on significant scale as a by-product of biodiesel manufacture and as such it is a promising alternative feedstock for the manufacture of valuable bulk chemicals from a bio-derived source [3]. Many processes for glycerol utilisation have been investigated in the last few years [3–6]. Derived chemicals include: glycerol carbonate, telomers, selective oxidation products, branched alkyl ethers, propanediols, epoxides, hydrocarbons and syngas, which can be converted to bulk chemicals and fuels. Glycerol hydrogenolysis to produce 1,2-propanediol has been widely studied [7–14]. Cu based catalysts are reported to show very high selectivity to 1,2-propanediol [11–14] and both gas phase and liquid phase processes for glycerol hydrogenolysis have been claimed [15]. These processes have the potential to provide a renewable and economic source of 1,2-propanediol.

Propionaldehyde is an important chemical intermediate used extensively in the manufacture of rubbers, plastics, paints, and pesticides. Currently, propionaldehyde is produced by petroleum-derived processes such as ethylene hydroformylation, propylene oxide isomerisation, and acrolein hydrogenation or as a by-product of acetone [16–19]. The ready availability of a process to produce

1,2-propanediol from glycerol, provides the opportunity for a two-step process to propionaldehyde from glycerol.

1,2-Propanediol dehydration readily occurs over electrophilic, nucleophilic and lanthanide oxide catalysts [20–31]. This reaction has been studied in the gas phase and in sub-, or supercritical water. Different products are obtained over the various catalysts according to the corresponding reaction mechanisms. Electrophilic catalysts are active in 1,2 elimination and favour propionaldehyde and acetone. Examples are catalysts such as heteropoly acids, Nafion-H, and NaHX. Mori et al. reported 100% conversion and 93 mol% selectivity to propionaldehyde for 1,2-propanediol dehydration over silica supported silicotungstic acid [24]. Nucleophilic catalysts can dehydrate 1,2-propanediol to propene oxide by attack on the primary hydroxyl proton. For example, 70% selectivity to propene oxide was reported over alkali metal loaded silica. In sub- and supercritical water, 80 mol% propionaldehyde yield was reported for 1,2-propanediol dehydration at 360 °C and 34 MPa with the addition of ZnSO_4 . Zeolite catalysts as solid acid catalysts have been widely studied for the dehydration of alcohols especially methanol and ethanol [32–35]. More recently, we have shown that zeolites are effective catalysts for dehydration of n-butanol [36], and in particular that the product distribution can be controlled by the shape selectivity arising from the unidirectional channel structure of ZSM-23 and Theta-1 (ZSM-22). In the context of glycerol conversion, zeolites have been used for dehydration to acrolein [37], and it has been reported recently that Theta-1 is also a highly selective catalyst for this reaction [38]. However, zeolite catalysts have not been studied previously for the dehydration of 1,2 propanediol to propionaldehyde although it is to be expected that they would prove to be efficient catalysts for this reaction.

* Corresponding author. Tel.: +44 0 20 7594 5579; fax: +44 0 20 7594 5637.
E-mail address: d.chadwick@imperial.ac.uk (D. Chadwick).

The present paper reports a study of the catalytic dehydration of 1,2-propanediol over a range of zeolite catalysts with different pore structures and acidities. Medium pore zeolites with unidirectional channels (ferrierite, Theta-1, ZSM-23) are compared with ZSM-5, which has 10-ring two-dimensional intersecting channels, and Y-zeolite, mordenite, and silica–alumina. All the zeolite catalysts are shown to be highly active for 1,2-propanediol dehydration. However, only the medium pore zeolites with unidirectional channels, namely Theta-1 and ZSM-23, are found to be highly selective for propionaldehyde.

2. Experimental

2.1. Catalysts

The H-form or NH_4 form of ferrierite ($\text{SiO}_2/\text{Al}_2\text{O}_3 = 20$ and 55), ZSM-5 ($\text{SiO}_2/\text{Al}_2\text{O}_3 = 50$ and 280), Y ($\text{SiO}_2/\text{Al}_2\text{O}_3 = 60$) and Mordenite ($\text{SiO}_2/\text{Al}_2\text{O}_3 = 20$) were purchased from Zeolyst. ZSM-23 ($\text{SiO}_2/\text{Al}_2\text{O}_3 = 68$) and Theta-1 ($\text{SiO}_2/\text{Al}_2\text{O}_3 = 63$) were synthesized according published literature [39,40]. The as-synthesised samples were calcined at 550°C using a very slow temperature ramp rate, exchanged with ammonium nitrate solution three times, and calcined again at 550°C to convert to the H-form. XRD was used to confirm the zeolite structures. These zeolite samples contained no binder and were granulated for the catalytic testing reported below. XRF was used to confirm the $\text{SiO}_2/\text{Al}_2\text{O}_3$ ratios. Silica–alumina and mordenite ($\text{SiO}_2/\text{Al}_2\text{O}_3 = 3.3$) were commercial catalysts containing binder.

The $\text{SiO}_2/\text{Al}_2\text{O}_3$ ratio of each of the zeolites was confirmed directly on the powder using a Bruker S4 explorer X-ray Fluorescence spectrometer. Surface areas and pore volumes were measured on a Micromeritics TriStar instrument using BET method. The pore volumes were calculated according to the procedure of Remy and Poncelet utilising the Dubinin and Radushkevich equation [41].

Ammonia temperature program desorption (TPD- NH_3) was carried out using a mass spectrometer detector. The desorbing ammonia was identified by $m/z = 16$. 0.1 g catalyst granules were loaded in a stainless steel reactor and pre-treated at 660°C in 40 ml/min He for 30 min. The temperature was decreased to 110°C , and ammonia was adsorbed to saturation over the catalyst. Ammonia was desorbed from 110 to 660°C at $10^\circ\text{C}/\text{min}$ in 40 ml/min He.

2.2. Catalyst activities

The catalysts were evaluated in a fixed-bed continuous flow microreactor system operating at ambient pressure. The zeolite powders were pressed (without addition of binder or lubricant) and sieved to form granules between 0.50 and 0.85 mm. A certain amount of the catalyst granules (0.05 g or 0.5 g) were diluted with inert silicon carbide granules of approximately the same size to make up a volume of 7.0 ml. The diluted catalyst was loaded into a tubular reactor (11 mm internal diameter), sandwiched between beds of inert granules. SiC was used as diluent because of its inertness and heat transfer properties, and the particle size, dilution ratio and pre/post packing were used to maintain plug flow and isothermality. The reaction was carried out between 200 and 400°C . The reactant was fed into the catalyst bed via an evaporator at 160°C , through which the gas diluent (argon) was passed. In some cases, a flow of steam was added to the inlet gas to the reactor. GHSV was defined with respect to the total gas volumetric flow and the undiluted catalyst volume. The WHSV of 1,2-propanediol, where given, was defined as mass flow of 1,2-propanediol/weight of undiluted catalyst. After passing through the catalyst, the prod-

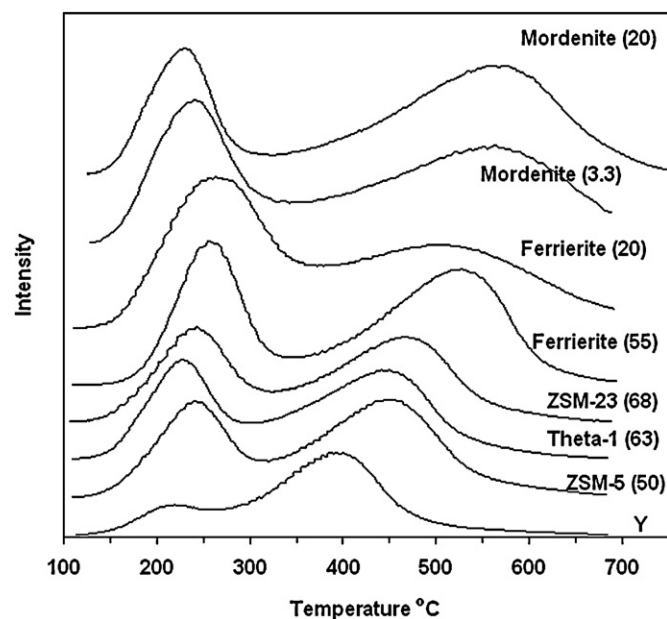


Fig. 1. Ammonia temperature programmed desorption (TPD NH_3) from the acid form of the zeolites.

uct was collected in a condenser kept at 0°C and the gas effluent was analysed by GC/FID using a Plot Al_2O_3 capillary column. The liquid product was collected and analysed by GC/FID using a HP-FFAP capillary column. A blank reaction at 300°C with only SiC diluent found a conversion of less than 1%. Carbon balances were $\pm 5\%$.

3. Results and discussion

The catalysts and their properties are listed in Table 1. In general, the zeolites used had $\text{SiO}_2/\text{Al}_2\text{O}_3$ ratios in the range of 50–68. Samples outside this range were included for the purposes of comparison. The mordenite and amorphous silica–alumina (ASA) compositions were as supplied commercially. The zeolites used were in the form of granulated powder and contained no binder, except for the mordenite (3.3) and the ASA which were commercial samples and contained a binder. The surface areas of the zeolites reported in Table 1 are consistent with literature values and the supplier data sheets. The micropore volumes are consistent with the structure of the zeolites and their framework densities [42–44].

The acid site densities were calculated from the $\text{SiO}_2/\text{Al}_2\text{O}_3$ ratios and are given in Table 1. The strength of the acid sites was determined by TPD- NH_3 . Profiles of the H-forms of the zeolites are shown in Fig. 1. All the zeolites exhibited two peaks, one at low temperature (LT) and the other at high temperature (HT). The HT was due to ammonia adsorbed on the Bronsted acid sites on the surface of the frameworks. The LT corresponded to ammonia hydrogen bonded to those adsorbed and contained within the micropores of the channels [45]. The temperatures corresponding to the HT peaks were characteristic of the strength of the acid site. As seen, the strength of the acid sites from TPD- NH_3 had the following trend: Mordenite \gg Ferrierite $>$ ZSM-23 \geq ZSM-5 \approx Theta-1 $>$ Y.

The zeolite composition and structural properties along with the reaction conditions strongly influenced the observed selectivities and thus the yield of propionaldehyde, which dominated at temperatures of 300°C and higher. 1,2-Diols are known to undergo the pinacol rearrangement to give the corresponding aldehyde [30]. A mechanism for 1,2-propanediol dehydration over acidic catalysts via E1 elimination is presented in Scheme 1. Protonation of either of the hydroxyl groups and rearrangement can produce three reactive carbenium intermediates (I, II, and III, Scheme 1), which yield ace-

Table 1
Catalysts and their properties.

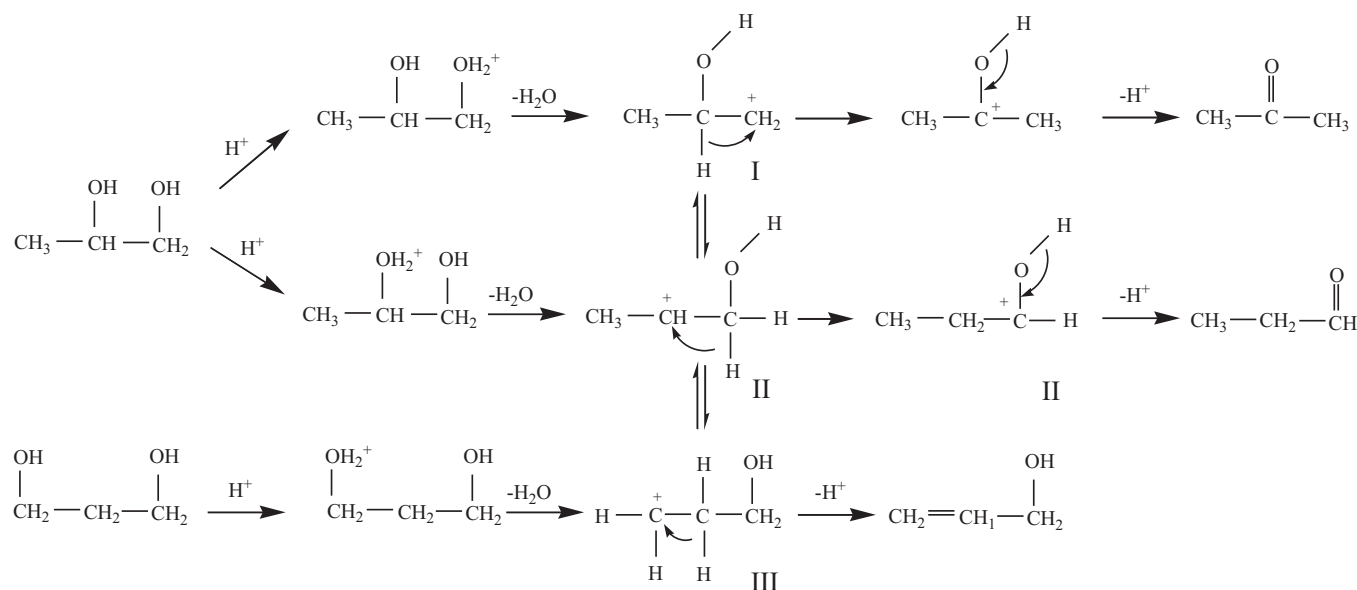
Catalyst	Type	SiO ₂ /Al ₂ O ₃	Channels ^c	S _{BET} (m ² /g)	Pore volume (cm ³ /g)	Acid site conc. (mmol H ⁺ /g) ^d
Silica-alumina ^b	–	1.3	–	364	0.082	–
Ferrierite(20)	FER	20	1D	367	0.148	1.54
Ferrierite (55)	FER	55	1D	323	0.130	0.59
ZSM-23(68)	MTT	68	1D	204	0.071	0.48
Theta-1(63)	TON	63	1D	208	0.079	0.52
Mordenite(20)	MOR	20	1D	399	0.158	1.54
Mordenite(3.3) ^b	MOR	3.3	1D	439	0.166	2.27 ^a
ZSM-5(50)	MFI	50	3D	408	0.175	0.64
ZSM-5(280)	MFI	280	3D	389	0.175	0.12
Y-zeolite(60)	FAU	60	3D	814	0.352	0.54

^a Assuming there is 25 wt% alumina binder.

^b Commercial and contains binder.

^c 1D 1 dimensional; 3D 3 dimensional.

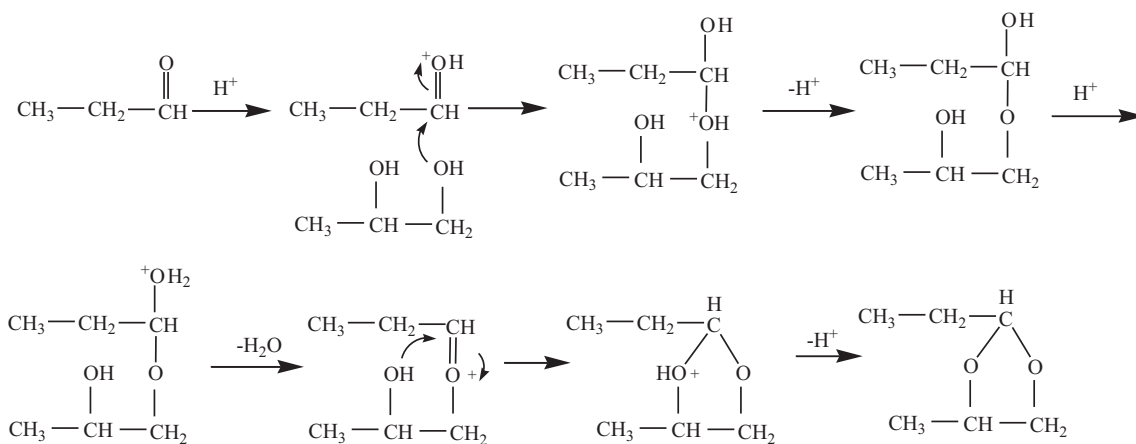
^d Calculated based on SiO₂/Al₂O₃.



Scheme 1. Propanediol dehydration over solid acid catalyst.

tone, propionaldehyde and allyl alcohol respectively. Carbenium ion (II) will have the highest concentration because the secondary carbenium ion is more stable than the primary carbenium ion. Thus, the main product of 1,2-propanediol dehydration is propionalde-

hyde. At much higher temperatures the activity for rearrangement leads to more by-products and a loss in selectivity to propionaldehyde. The main side products formed were acetone, allyl alcohol, propanol, hydrocarbons (mainly propene), and 2-ethyl-4-methyl-



Scheme 2. Formation of 2-ethyl-4-methyl-1,3-dioxolane.

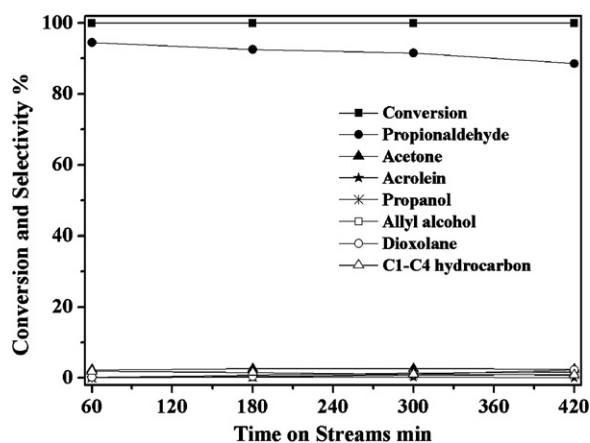


Fig. 2. 1,2-Propanediol dehydration over ZSM-23(68); $T = 300\text{ }^{\circ}\text{C}$, GHSV = $45,000\text{ h}^{-1}$, 1,2-propanediol mole fraction = 0.027.

1,3-dioxolane (referred to here as dioxolane for brevity) at the lower temperatures. Dioxolane is produced from reaction of 1,2-propanediol with propionaldehyde [24]. The probable reaction mechanism is presented in Scheme 2. Hemiacetal can be produced from addition of the primary hydroxyl group of 1,2-propanediol to the formed propionaldehyde. The formed hemiacetal can undergo intra-molecular addition with the secondary hydroxyl group to form acetal (2-ethyl-4-methyl-1,3-dioxolane). Propanol is believed to form by hydrogen addition, most probably via hydrogen transfer from a diol or intermediate to propionaldehyde and, as the formation of dioxolane, it is a bi-molecular reaction. When intermolecular hydrogen transfer occurs, highly unsaturated hydrocarbons are formed such as dienes, alkynes and coke.

1,3-Propanediol can also form the carbenium intermediates I, II, and III, Scheme 1. 1,3-propanediol dehydration is more difficult than 1,2-propanediol dehydration because of the relative stabilities of carbenium ions (III) and (II). Product selectivity for 1,3-propanediol depends on competition between deprotonation and carbenium ion rearrangement: at lower temperatures carbenium ion (III) mainly deprotonates directly to form allyl alcohol, but at higher reaction temperatures carbenium ion rearrangement leads to a range of other products including propanol, propene, acrolein and propionaldehyde.

3.1. Effect of reaction temperature on 1,2-propanediol dehydration

The time-on-stream performance at a 1,2-propanediol partial pressure of 0.027 was studied over a period of 7 h for ZSM-23. Results at $300\text{ }^{\circ}\text{C}$ are given in Fig. 2. The conversion was stable over this time period and selectivity to propionaldehyde only dropped marginally. Consequently, data was collected at this partial pressure as a function of temperature.

Alcohol dehydration is favoured at higher temperatures. Furthermore, some side reactions such as self-reaction of aldehydes and ketones as well as olefins/dienes polymerisation are less favoured at high temperature. Fig. 3 shows the conversions and product distributions of 1,2-propanediol dehydration over ZSM-23 from 200 to $400\text{ }^{\circ}\text{C}$. As seen the conversion rapidly increased with increasing temperature approaching 100% at a temperature $> 250\text{ }^{\circ}\text{C}$. At low temperature ($200\text{ }^{\circ}\text{C}$) the conversion was low and most of the selectivity was to the formation of dioxolane. Very high selectivity to propionaldehyde was obtained at $300\text{--}350\text{ }^{\circ}\text{C}$. Further increase in the temperature (to $400\text{ }^{\circ}\text{C}$) resulted in formation of acetone at the expense of the propionaldehyde, although at all the studied temperatures the selectivity to acrolein, allyl

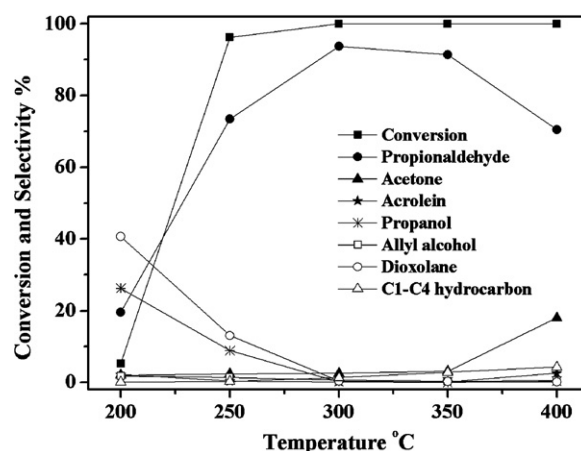


Fig. 3. Effect of temperature on 1,2-propanediol dehydration over ZSM-23(68); GHSV = $45,000\text{ h}^{-1}$, 1,2-propanediol mole fraction = 0.027, temperature = $200\text{--}400\text{ }^{\circ}\text{C}$.

alcohol, and acetone were always low. Similar trends of temperature dependency of selectivity were shown by all the catalysts although the absolute level of selectivity depended strongly on the zeolite structure as discussed in more detail below and the onset of deactivation at the highest temperature for the more acidic catalysts probably takes place. The overall behaviour is consistent with the mechanisms presented in Schemes 1 and 2.

3.2. Influence of the zeolite type on the performance

The performance over the catalysts at the same temperature was found to depend primarily on the pore structure of the catalyst. Results obtained at 250 and $300\text{ }^{\circ}\text{C}$ and a 1,2-propanediol partial pressure of 0.027 are given in Table 2. At these temperatures and partial pressure the effect of deactivation was minimal over the reaction time except for the most acidic catalyst (mordenite(20)). All the zeolites were more active than the commercial silica–alumina reflecting the higher acidity provided by the zeolitic structure. The conversion levels over the zeolites reached in excess of 95% and mostly approached complete conversion at the higher temperatures applied. The selectivity, on the other hand, was strongly influenced by the pore structure and acid strength of the zeolite. The best selectivities for the production of propionaldehyde were obtained over zeolites with intermediate acidity (acid strength as evaluated from the TPD-NH₃, see Fig. 1 and trend above) and medium pore, unidirectional channels as shown in Table 2. These are represented by Theta-1 and ZSM-23 which gave selectivities in excess of 93 wt%. ZSM-5(50) which had similar acid strength to Theta-1 but with intersecting channels, gave a high, but lower selectivity. The differences in conversion and selectivity between Theta-1, ZSM-23 and ZSM-5(50) may also reflect the subtle changes in channel shape from elliptical or pear-shape to more circular respectively. Zeolites with higher acidity and near circular channels such as Ferrierite or large pores such as mordenite gave lower selectivities. Y zeolite with lower acidity and larger pores also gave inferior selectivity.

Formation of dioxolane from propionaldehyde and 1,2-propanediol is a bi-molecular reaction which appears to require cage-like channels, since ferrierite, ZSM-5, mordenite and Y zeolite all gave higher selectivity for dioxolane production at $250\text{--}300\text{ }^{\circ}\text{C}$ than ZSM-23 and Theta-1, Table 2. This was particularly evident at $250\text{ }^{\circ}\text{C}$, as the concentration of the 1,2-propanediol was higher and its reaction with the propionaldehyde was more favourable. Theta-1 and ZSM-23, on the other hand, restrict the production

Table 2
1,2-Propanediol dehydration over zeolite catalysts^a.

Catalyst ^b	T, °C	Conversion, %	Selectivity, wt%								
			Propionaldehyde	Acetone	Acrolein	Propanol	Allyl alcohol	Dioxolane	Propene	Other hydrocarbons	Others
Silica–alumina	300	57.6	62.8	7.1	0.3	3.9	1.4	5.4	1.8	0.1	17.2
Ferrierite(20)	300	98.9	77.8	4.1	0.5	2	1.3	6.8	0.7	–	6.8
	250	83.2	29.1	1.2	0.4	25.5	1.3	39.1	0.1	–	3.3
Ferrierite(55)	300	81.7	64.9	2.5	0.3	8.1	2.5	10.3	1.1	0.1	10.1
	250	51.4	29.7	0.5	0	29.5	0.2	36	0.3	–	3.8
ZSM-23(68)	300	100	93.8	2.6	0.2	0.2	0.6	0.4	1.3	–	0.9
	250	96.2	73.5	2.4	0.3	8.8	1.4	13.1	0.3	–	0.2
Theta-1(63)	300	100	93.4	2.2	0.3	0.1	0.4	0.2	2.1	–	1.3
	250	99.1	80.6	2.3	0.2	5.3	1.3	8.5	0.6	–	1.2
ZSM-5(50)	300	99.2	88.1	2.3	0.2	1.2	1.4	2.3	1.2	0.1	3.2
	250	92.4	67.6	0.8	0	10.3	0.1	13	0.3	0.1	7.8
ZSM-5(280)	300	90.4	70.6	1.9	0.1	4.0	2.1	7.4	1.3	–	12.6
	250	82.4	43.7	1.5	0.1	20	0.2	25.8	0.3	–	8.4
Mordenite(3.3)	300	95.3	64.3	9.3	0.5	2.6	2.9	4.2	0.3	0.1	15.8
	250	17.5	23.6	4.4	0	20.2	3	31.4	0.1	0.1	17.2
Y-zeolite(60)	300	96.9	70.9	3.8	0.3	5.3	1.7	12.7	1.2	0.1	4.0
	250	81.5	30.7	1.8	0.3	22.3	0.3	30.9	1	0.1	12.8

^a GHSV = 45,000 h⁻¹; WHSV (1,2-propanediol) = 8.2 g g⁻¹ h⁻¹; 1,2-propanediol mole fraction = 0.027.

^b SiO₂/Al₂O₃ ratios given in parentheses.

of dioxolane owing to their transition state shape selectivity. A competing reaction is the formation of acetone, which requires protonation of the alcohol group on the primary carbon and formation of primary carbenium ion as in Scheme 1 and discussed above. The selectivity for acetone production was similar in Theta-1, ZSM-23, ZSM-5(50) and ferrierite(55) and highest in the case of mordenite, silica–alumina and ferrierite(20) catalysts, as shown in Table 2. With the exception of Y zeolite, it suggests that increased selectivity to acetone is associated with a high density of acid sites on the surface of the catalysts.

It is worth noting that the formation of propanol requires hydrogen transfer activity, which is, as in the formation of dioxolane, a bi-molecular reaction. It is normally promoted by low SiO₂/Al₂O₃ (i.e. denser acid sites) and relatively larger pore size. The levels of propanol reported in Table 2 for the various catalysts are consistent with this trend, as the highest propanol levels were achieved with Y, silica–alumina, mordenite, and ferrierite. Zeolite Y and silica–alumina are known for their high hydrogen transfer activity, a property which makes them good commercial catalyst for FCC where hydrogen redistribution is highly desirable. As the formation of dioxolane and propanol require similar catalyst characteristics, their formation is linked to the same catalyst properties. Graphical correlation of the two products confirmed this as shown in Fig. 4(a). Propanol can be converted further by dehydration to propene. A plot of dioxolane versus propanol + propene is shown in Fig. 4(b). Again it shows a good correlation except that in some cases significant propene is observed when the dioxolane selectivity falls to a very low value. This suggests the further conversion of dioxolane which is discussed below.

The formation of dioxolane and the loss of selectivity to dioxolane is an interesting feature of the product distributions in Table 2. In addition to the catalyst structure and temperature dependence seen in Table 2 and discussed above there is a general trend to lower selectivity to dioxolane with increasing conversion. To investigate this aspect, the selectivity to dioxolane at a lower space velocity was investigated over ferrierite(20), bound mordenite(3.3) and commercial silica–alumina, as these catalysts had relatively high selectivity to dioxolane even at 300 °C (see Table 2). The lower GHSV of 4500 h⁻¹ was achieved by increasing the volume of catalyst (decreasing the dilution to keep the same catalyst bed total volume) at the same feed partial pressures and flow rate. The results are given in Table 3. As expected, the conversion of 1,2-propanediol increased at lower GHSV reaching 100% over all three

catalysts. At the lower GHSV the selectivity to dioxolane decreased almost to zero while the selectivity to propionaldehyde increased. The disappearance of dioxolane from the products was most probably due to a combination of two factors: the low concentration of 1,2-propanediol at such a high conversion and the further reaction of any dioxolane that formed. The presence of 1,2-propanediol is essential for the formation of dioxolane as shown in Scheme 2. The parallel rise in selectivity to propionaldehyde (and to a lesser extent acetone) at the longer residence time suggests that dioxolane decomposes over acidic catalysts to yield propionaldehyde (also noted by Mori et al. [24]). At lower reaction temperatures, propionaldehyde appears to be formed by two routes: by direct protonation/dehydration as shown in Scheme 1, and via the decomposition of dioxolane which formed according to Scheme 2. As the reaction temperature is increased to 300 °C and above, the production of dioxolane is suppressed. This is probably associated with the effects of configurational diffusion and shape selectivity and it is expected that the direct protonation/dehydration route becomes the main pathway to propionaldehyde.

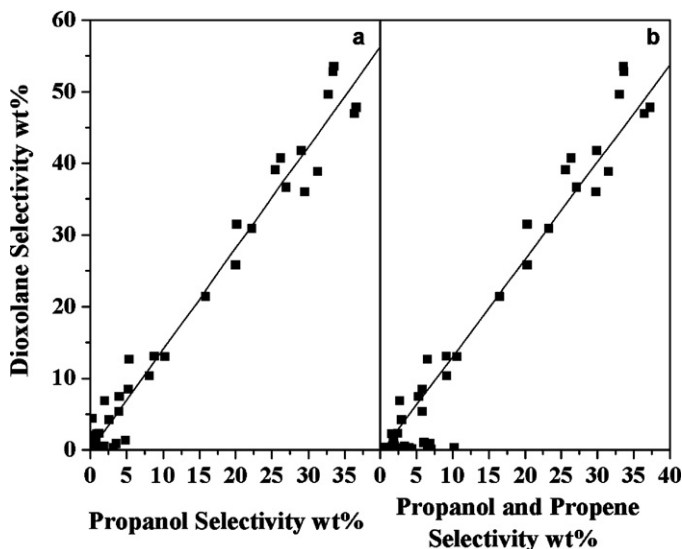


Fig. 4. Correlation of selectivity to dioxolane with (a) propanol, (b) propanol + propene; GHSV = 45,000 h⁻¹, 1,2-propanediol mole fraction = 0.027, temperature = 200–400 °C.

Table 3
Dehydration of 1,2-propanediol at lower GHSV^a.

Catalyst	T, °C	Conversion, %	Selectivity, wt%								
			Propionaldehyde	Acetone	Acrolein	Propanol	Allyl alcohol	Dioxolane	Propene	Other hydrocarbons	others
Silica–alumina ^b	250	100	53.8	5.3	0.2	15.6	2.9	6.5	1.9	–	13.8
	300	100	70.2	8.4	0.3	6.1	0.3	0	7.3	0.3	7.1
Ferrierite(20)	250	100	92.1	6.0	0.1	0.8	0	0	0.8	0.2	0
	300	100	82.9	11.8	2.7	1.0	0	0	1.2	0.3	0.1
Mordenite(3.3) ^b	250	100	63.7	12.5	0	10.3	0	0	0.8	0.2	12.5
	300	100	70.0	15.7	0.1	4.9	1.1	0.1	2.4	1.0	4.7

^a GHSV = 4,500 h⁻¹, 1,2-propanediol mole fraction = 0.027.^b Commercial samples containing binder.

Similar results on the space velocity dependence of the selectivity to dioxolane were reported by Mori et al. for heteropoly acid catalysts [24]. The study was done mainly at a lower space velocity (GHSV of approximately 6000 h⁻¹). Allowing for the generally lower reaction temperatures used in their study, it would appear that the zeolite catalysts have broadly similar activity while achieving a similar maximum selectivity to propionaldehyde. Zeolites and in particular ZSM-23, Theta-1 and ZSM-5 offer in addition inherent selectivity and stability to cyclic regeneration.

Binderless mordenite(20) gave a similar trend in terms of dioxolane/propionaldehyde selectivities as a function of temperature, but gave a poor mass balance suggesting greater coke formation and consistent with the high acidity of this catalyst, Fig. 1.

3.3. Effect of zeolite silica/alumina ratio

The number of acid sites is determined by the silica/alumina ratio, whereas the strength of the acid site depends on its degree of isolation and structural environment. The effect of zeolite silica/alumina ratio was studied for two zeolites with unidirectional channels and intersecting channels respectively for which a wide range values is readily available commercially, namely ferrierite ((20) and (55)), and ZSM-5 ((50) and (280)). Figs. 5 and 6 show conversion and selectivity to selected products as a function of temperature. Both ferrierite and ZSM-5 show that the higher SiO₂/Al₂O₃ ratio catalyst was less active than the zeolite with lower SiO₂/Al₂O₃ ratio at all temperatures, which was consistent with the lower density of acid sites. However, the impact on the conversion is not so great and suggests that the turnover per acid site is greater for

the zeolites with higher SiO₂/Al₂O₃ ratio. Higher propionaldehyde selectivity is observed over the zeolite with lower SiO₂/Al₂O₃ ratio at the same temperature, but the selectivity to propionaldehyde reaches a maximum at a higher temperature for the higher acid concentration catalysts. The bi-molecular reaction to dioxolane is suppressed at higher temperatures as discussed above and at 400 °C and above the selectivity to a range of products including acetone, allyl alcohol, acrolein, propene and higher hydrocarbons increased as expected from Scheme 1, but the onset of deactivation cannot be excluded.

3.4. Effect of steam and oxygen on 1,2-propanediol dehydration

ZSM-23 and Theta-1 which have similar channel structure were found to be the most selective and active catalysts for propionaldehyde production. Consequently, ZSM-23 was used to study conversion at a higher partial pressure of 1,2-propanediol, and the effect of added steam and/or oxygen. The time-on-stream performance of ZSM-23 at the low 1,2-propanediol partial pressure of 0.027 was found to be stable as reported above. However, with an almost 10 fold increase in the partial pressure (from 0.027 to 0.22), significant deactivation with time-on-stream took place as seen in Fig. 7: the conversion dropped from 100% to 20% in 3 h at 300 °C and the propionaldehyde selectivity also decreased. The selectivity to dioxolane and propanol increased, probably in the former case due to the increased partial pressure providing 1,2-propanediol for the reaction with propionaldehyde. Catalyst deactivation also resulted in higher formation of hydrocarbons, propene and most probably dienes and alkynes. Increasing the temperature to 400 °C

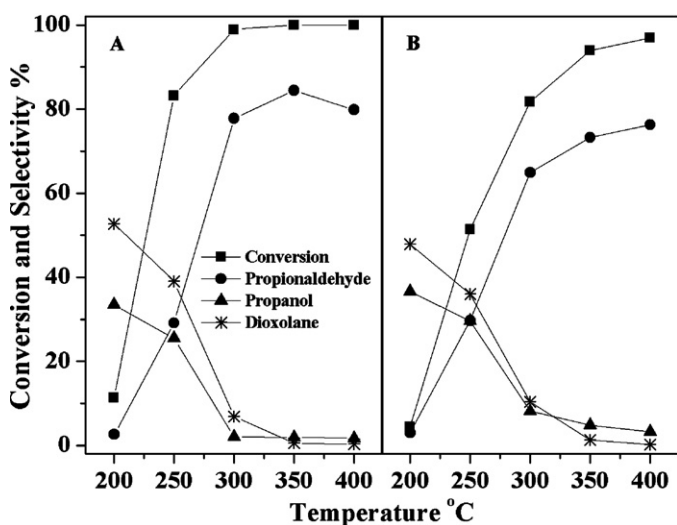


Fig. 5. Effect of silica/alumina ratio of ferrierite on 1,2-propanediol dehydration. GHSV = 45,000 h⁻¹, 1,2-propanediol mole fraction = 0.027. (A) Ferrierite(20), (B) Ferrierite(55), temperature = 200–400 °C.

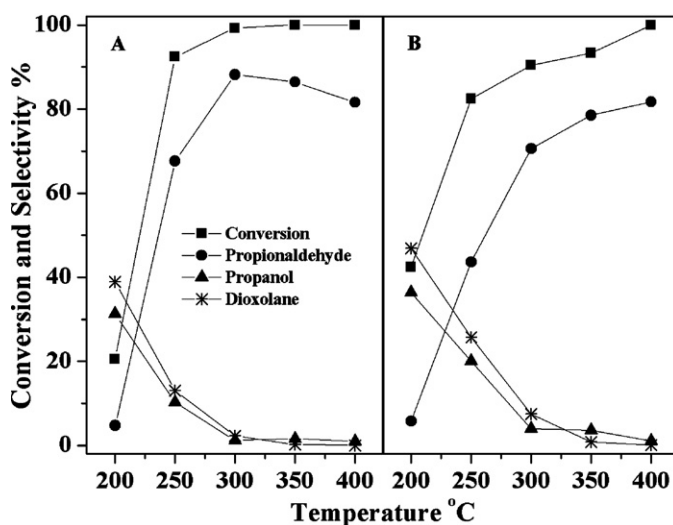


Fig. 6. Effect of silica/alumina ratio of ZSM-5 on 1,2-propanediol dehydration. GHSV = 45,000 h⁻¹, 1,2-propanediol mole fraction = 0.027, temperature = 200–400 °C. (A) ZSM-5(50), (B) ZSM-5(280).

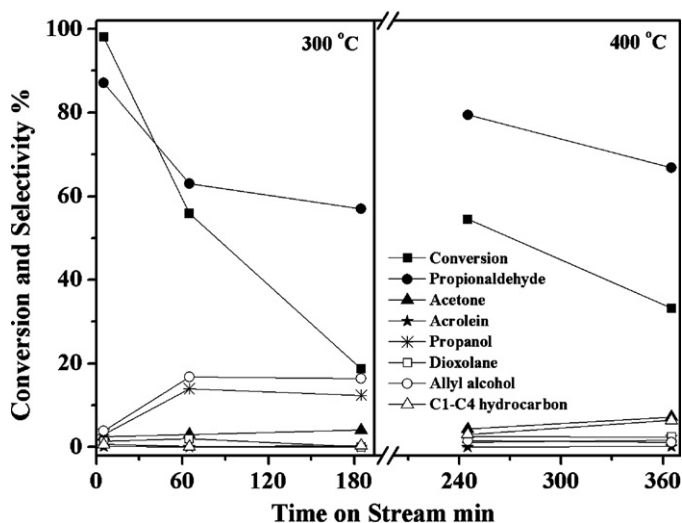


Fig. 7. 1,2-Propanediol dehydration over ZSM-23(68) at higher reactant partial pressure. GHSV = 56,000 h⁻¹, 1,2-propanediol mole fraction = 0.22, temperature = 300 and 400 °C.

had an impact on the performance increasing the conversion and the selectivity to propionaldehyde. This suggested that the initial deactivation was partly associated with relatively low molecular weight hydrocarbons, which evaporated or gasified in the product steam at higher temperature. At 400 °C the deactivation rate continued but not quite as steeply as experienced at lower temperature. While the higher temperature resulted in a decrease in the selectivity to dioxolane and propanol, the selectivity to hydrocarbons noticeably increased. ZSM-5 had a similar time-on-stream trend to ZSM-23. At 300 °C the level of dioxolane and propanol were found to be higher as expected from the more open structure of ZSM-5 relative to ZSM-23.

In an industrial process, steam is a convenient diluent. Water is also a co-product of 1,2-propanediol dehydration, and using steam as diluent simplifies the separation and recycle processes. Furthermore in view of the deactivation reported above for higher 1,2-propanediol partial pressure, addition of steam may suppress the coke formation and improve performance with the time-on-stream. Steam has been widely reported to reduce the formation rate of coke over solid acid catalysts [46–48]. To investigate this, the

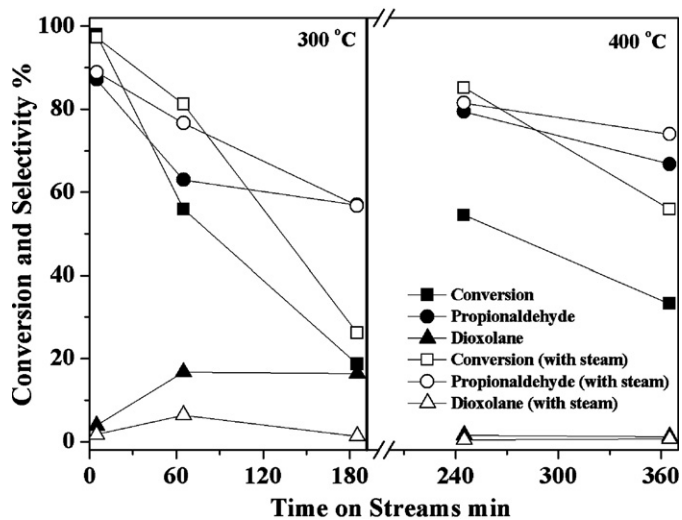


Fig. 8. Effect of steam on 1,2-propanediol dehydration over ZSM-23(68). GHSV = 56,000 h⁻¹, 1,2-propanediol mole fraction = 0.22, steam mole fraction = 0.27, temperature = 300 and 400 °C.

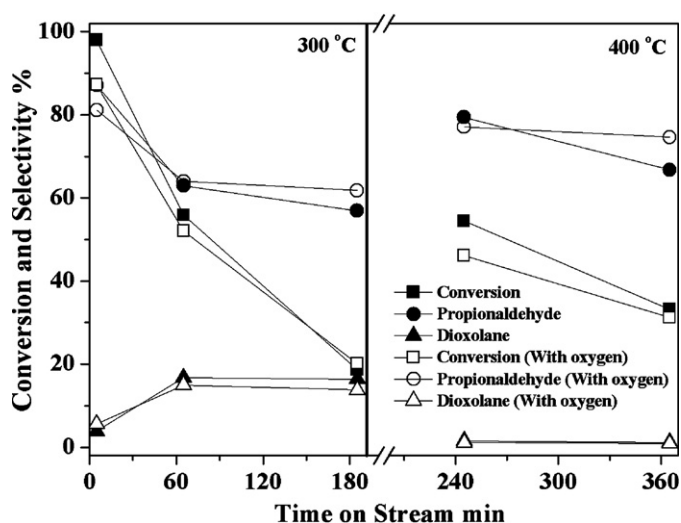


Fig. 9. Effect of oxygen addition on 1,2-propanediol dehydration over ZSM-23(68). GHSV = 56,000 h⁻¹, 1,2-propanediol mole fraction = 0.22, oxygen mole fraction = 0.03, temperature = 300 and 400 °C.

effect of steam on 1,2-propanediol dehydration was studied over ZSM-23(68) and ZSM-5(50). The results for ZSM-23(68) with and without steam are shown in Fig. 8. In the presence of steam, a substantial improvement in the performance with time-on-stream was obtained for both zeolites. The increase in conversion and selectivity to propionaldehyde over ZSM-23(68) compared to when steam was not present is clearly seen in Fig. 8. Thus, adding steam into the reaction system is practical and mitigates the deactivation. Mori et al. studied the effect of steam on 1,2-propanediol dehydration over heteropoly acid catalysts [24], and also found that steam at diol/steam ratios of 0.1–1 was effective in increasing conversion and also selectivity to propionaldehyde. However, in their study the addition of steam simultaneously decreased the partial pressure of 1,2-propanediol in the gas phase, and as we have shown, using lower 1,2-propanediol partial pressure also increases conversion and the selectivity to propionaldehyde, and gives improved catalyst stability. The present results with added steam were achieved at constant 1,2-propanediol partial pressure. However, the effect of steam was broadly similar to that reported by Mori et al. [24].

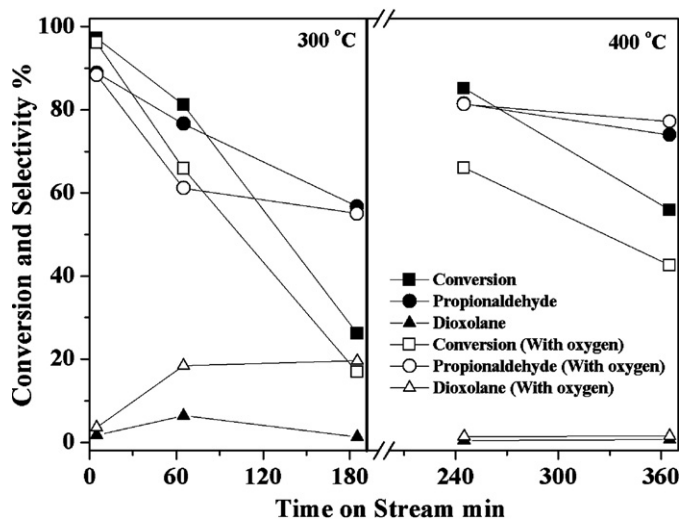


Fig. 10. Effect of oxygen and steam addition on 1,2-propanediol dehydration over ZSM-23(68). GHSV = 56,000 h⁻¹, 1,2-propanediol mole fraction = 0.22, steam mole fraction = 0.27, oxygen mole fraction = 0.03, temperature = 300 and 400 °C.

Figs. 9 and 10 show the effect of oxygen addition on 1,2-propanediol over ZSM-23(68) at the higher 1,2-propanediol mole fraction (0.22) in the absence and in the presence of steam (mole fraction at 0.27) respectively. The total GHSV was kept constant at 56,000 h⁻¹. Addition of oxygen has been reported to inhibit formation of by-products and catalyst deactivation in glycerol dehydration over solid acid [49]. As seen in Figs. 9 and 10, the addition of oxygen does not show the expected beneficial effect.

4. Conclusions

Zeolite catalysts were found to be highly active for the dehydration of 1,2-propanediol yielding propionaldehyde with high selectivity at 300–350 °C. Zeolites with non-intersecting, unidirectional channels gave the highest selectivity to propionaldehyde which is interpreted as being due to their transition state shape selectivity suppressing the bi-molecular side reactions that can lead to the formation of 2-ethyl-4-methyl-1,3-dioxolane and propanol. For example, ZSM-23 and Theta-1, gave complete conversion and over 93 wt% selectivity to propionaldehyde at 300 °C corresponding to a productivity of about 7.5 kg/kg-cat/h. 2-ethyl-4-methyl-1,3-dioxolane was the main product at lower reaction temperatures, around 200 °C, and high GHSV. Decreasing GHSV reduced the selectivity to dioxolane which is interpreted as being due to the further conversion of dioxolane, mainly to propionaldehyde. The formation of dioxolane and propanol (and propene) was linked to the same catalyst properties and their production was shown to be correlated over the catalysts in this study.

Lower reactant partial pressure gave greater selectivity to propionaldehyde. In the catalysts where the SiO₂/Al₂O₃ ratio was varied, ZSM-5 and ferrierite, higher SiO₂/Al₂O₃ ratio gave greater selectivity to propionaldehyde. Faster deactivation was observed when operating at high partial pressures of 1,2-propanediol. Adding steam to the feed mitigated the deactivation to a significant extent, but did not suppress it completely. The results suggest that a two-step process from glycerol to propionaldehyde via 1,2-propanediol could be attractive.

Acknowledgements

We thank the Technology Strategy Board (UK) for financial support under the Moving to Zero Emissions Programme and Raul Montesano for assistance with the TPD.

References

- [1] A.K. Agarwal, Prog. Energy Combust. Sci. 33 (2007) 233–271.
- [2] F.R. Ma, M.A. Hanna, Bioresour. Technol. 70 (1999) 1–15.
- [3] A. Behr, J. Eilting, K. Irawadi, J. Leschinski, F. Lindner, Green Chem. 10 (2008) 13–30.
- [4] D.T. Johnson, K.A. Taconi, Environ. Prog. 26 (2007) 338–348.
- [5] Y.G. Zheng, X.L. Chen, Y.C. Shen, Chem. Rev. 108 (2008) 5253–5277.
- [6] C.H.C. Zhou, J.N. Beltramini, Y.X. Fan, G.Q.M. Lu, Chem. Soc. Rev. 37 (2008) 527–549.
- [7] K.Y. Wang, M.C. Hawley, S.J. DeAthos, Ind. Eng. Chem. Res. 42 (2003) 2913–2923.
- [8] M. Pagliaro, R. Ciriminna, H. Kimura, M. Rossi, C. Della Pina, Eur. J. Lipid Sci. Technol. 111 (2009) 788–799.
- [9] M.A. Dasari, P.P. Kiatsimkul, W.R. Sutterlin, G.J. Suppes, Appl. Catal. A: Gen. 281 (2005) 225–231.
- [10] J. Chaminand, L. Djakovitch, P. Gallezot, P. Marion, C. Pinel, C. Rosier, Green Chem. 6 (2004) 359–361.
- [11] L.Y. Guo, J.X. Zhou, J.B. Mao, X.W. Guo, S.G. Zhang, Appl. Catal. A: Gen. 367 (2009) 93–98.
- [12] Z.W. Huang, F. Cui, H.X. Kang, J. Chen, C.G. Xia, Appl. Catal. A: Gen. 366 (2009) 288–298.
- [13] C.H. Liang, Z.Q. Ma, L. Ding, J.S. Qiu, Catal. Lett. 130 (2009) 169–176.
- [14] J. Zheng, W.C. Zhu, C.X. Ma, M.J. Jia, Z.L. Wang, Y.H. Hou, W.X. Zhang, Polish J. Chem. 83 (2009) 1379–1387.
- [15] P. O'Connor, A.C. Corma, G. Huber, A.L. Savanaud, WO Pat., 052 993, 2008.
- [16] M.W. Balakos, S.S.C. Chuang, J. Catal. 151 (1995) 253–265.
- [17] M. Bron, D. Teschner, A. Knop-Gericke, F.C. Jentoft, J. Krohnert, J. Hohmeyer, C. Volckmar, B. Steinhauer, R. Schlögl, P. Claus, Phys. Chem. Chem. Phys. 9 (2007) 3559–3569.
- [18] T. Imanaka, S. Teranishi, Y. Okamoto, Bull. Chem. Soc. Jpn. 45 (1972) 1353.
- [19] V.I. Zapirtan, B.L. Mojert, J.G. van Ommen, J. Spitzer, L. Lefferts, Catal. Lett. 101 (2005) 43–47.
- [20] I. Bucsi, A. Molnar, M. Bartok, G.A. Olah, Tetrahedron 51 (1995) 3319–3326.
- [21] Z.Y. Dai, B. Hatano, H. Tagaya, Appl. Catal. A: Gen. 258 (2004) 189–193.
- [22] R.S. Düsselkamp, B.D. Harris, J.N. Patel, T.R. Hart, C.H.F. Peden, Inorg. Chem. Commun. 11 (2008) 561–563.
- [23] V. Lehr, M. Sarlea, L. Ott, H. Vogel, Catal. Today 121 (2007) 121–129.
- [24] K. Mori, Y. Yamada, S. Sato, Appl. Catal. A: Gen. 366 (2009) 304–308.
- [25] L. Ott, V. Lehr, S. Urfels, M. Bicker, H. Vogel, J. Supercrit. Fluids 38 (2006) 80–93.
- [26] C. Rungnim, V. Ruangpornvisuti, J. Comput. Chem. 26 (2005) 1592–1599.
- [27] S. Sato, R. Takahashi, T. Sodesawa, N. Honda, H. Shimizu, Catal. Commun. 4 (2003) 77–81.
- [28] S. Sato, R. Takahashi, T. Sodesawa, N.T. Honda, J. Mol. Catal. A: Chem. 221 (2004) 177–183.
- [29] G. Speranza, W. Buckel, B.T. Golding, J. Porph. Phthal. 8 (2004) 290–300.
- [30] B. Torok, I. Bucsi, T. Beregszaszi, I. Kapocsi, A. Molnar, J. Mol. Catal. A: Chem. 107 (1996) 305–311.
- [31] Z.X. Yu, L. Xu, Y.X. Wei, Y.L. Wang, Y.L. He, Q.H. Xia, X.Z. Zhang, Z.M. Liu, Chem. Commun. (2009) 3934–3936.
- [32] J.D. Bi, X.W. Guo, M. Liu, X.S. Wang, Catal. Today 149 (2010) 143–147.
- [33] H. Chiang, A. Bhan, J. Catal. 271 (2010) 251–261.
- [34] N. Khandan, M. Kazemeini, M. Aghaziarati, Appl. Catal. A: Gen. 349 (2008) 6–12.
- [35] K. Ramesh, C. Jie, Y.F. Han, A. Borgna, Ind. Eng. Chem. Res. 49 (2010) 4080–4090.
- [36] D. Zhang, R. Al-Hajri, S.A.I. Barri, D. Chadwick, Chem. Commun. 46 (2010) 4088–4090.
- [37] C.J. Jia, Y. Liu, W. Schmidt, A.H. Lu, F. Schuth, J. Catal. 269 (2010) 71–79.
- [38] T.Q. Hoang, X.L. Zhu, T. Danuthai, L.L. Lobban, D.E. Resasco, R.G. Mallinson, Energy Fuels 24 (2010) 3804–3809.
- [39] S.A.I. Barri, P. Howard, C.D. Telford, EU Pat., 0 057 049, 1982.
- [40] S.A.I. Barri, GB Pat., 2 190 910, 1987.
- [41] M.J. Remy, G. Poncelet, J. Phys. Chem. 99 (1995) 773–779.
- [42] S.A.I. Barri, G.W. Smith, D. White, D. Young, Nature 312 (1984) 533–534.
- [43] P.A. Wright, J.M. Thomas, R.G. Millward, S. Ramdas, S.A.I. Barri, J. Chem. Soc. Chem. Commun. 16 (1985) 1117–1119.
- [44] D. Breck, Zeolite Molecular Sieves: Structure, Chemistry and Use, J. Wiley, 1973.
- [45] N. Katada, H. Igi, J. Kim, M. Niwa, J. Phys. Chem. B 101 (1997) 5969–5977.
- [46] C.A. Bernardo, D.L. Trimm, Carbon 17 (1979) 115–120.
- [47] A.G. Gayubo, A.T. Aguayo, A.E.S. del Campo, P.L. Benito, J. Bilbao, in: B. Delmon, G.F. Froment (Eds.), Catalyst Deactivation, vol. 126, Elsevier, Amsterdam, 1999, pp. 129–136.
- [48] Y.X. Zhao, F. Wei, Y. Yu, Chin. J. Chem. Eng. 16 (2008) 726–732.
- [49] J.L. Dubois, C. Duquenne, W. Holderich, US Pat., 7 396 962 B1, 2008.